Journal of Institute of Science and Technology, 29(2), 95-108 (2024)
ISSN: 2467-9062 (print), e-ISSN: 2467-9240
https://doi.org/10.3126/jist.v29i2.67919

Research Article

INHIBITORY ACTIVITY OF MYRICETIN AND CHLOROGENIC ACID AGAINST DENGUE VIRUS NS2B/NS3 PROTEASE THROUGH *IN SILICO* APPROACHES

Nirajana Dhoju, Tika Ram Lamichhane*

Central Department of Physics, Institute of Science and Technology, Tribhuvan University, Kirtipur, Kathmandu, Nepal
**Correspondence: tika.lamichhane@cdp.tu.edu.np*

(Received:** July 17, 2024; **Final Revision:** December 20, 2024**; Accepted:** December 22, 2024**)

ABSTRACT

The resurgence of dengue virus (DENV) infection poses a significant global health threat, exacerbated by urbanization and climate change. Flaviviridae family virus, DENV infection can be asymptomatic in some cases while it can be lethal in others. More serious symptoms include dengue hemorrhagic fever, dengue shock syndrome, and liver damage. Despite these worrying features, no specific drug has been approved till now. People have been relying on antipyretic drugs only. This study explores the inhibition potential of natural compounds myricetin and chlorogenic acid against DENV using computational analysis. Molecular docking and molecular dynamics simulations were employed to assess their inhibitory effects on a crucial enzyme NS2B/NS3 protease of DENV. NS2B/NS3 protease, highly conserved in the DENV serotypes, plays a vital role in viral replication and it acts as an excellent drug target. The phytochemicals myricetin (MYR) and chlorogenic acid (CGA) have docking scores of -7.9 kcal/mol and -7.1 kcal/mol targeting NS2B/NS3 protease, respectively. By analyzing RMSD, RMSF, RG, SASA and H-bonding, MYR possesses greater compactness and stability in comparison with quercetin and CGA throughout the MD simulation. The NS2B/NS3 protease in complex with MYR and CGA shows end-state MM/GBSA free energy of -25.05±3.19 kcal/mol and -20.22±3.02 kcal/mol, respectively. ADMET analysis shows that the proposed compounds offer good bioavailability scores. CGA with a higher LD50 value (5000 mg/kg) appears in predicted toxicity class 5 whereas quercetin and MYR with lower LD50 value (159 mg/kg) appear in the toxicity class 3. The results suggest that CGA and MYR exhibit strong binding affinities and stable interactions, highlighting their potential as DENV inhibitors. Further experimental verifications will be necessary to determine the effectiveness of such drug candidates against DENV.

Keywords: Chlorogenic acid, dengue virus, molecular docking, molecular dynamics, myricetin, NS2B/NS3 protease

INTRODUCTION

Dengue virus (DENV) is a mosquito-borne flavivirus that causes significant morbidity and mortality globally. A Chinese medical encyclopedia published the earliest description of clinically compatible sickness in 992 AD. The main mosquito vector, Aedes aegypti, found perfect circumstances as port towns thrived and became more urbanized throughout the 18th and 19th centuries as the global shipping sector expanded. As a result, the viruses and mosquitoes spread to other regions, culminating in substantial outbreaks. However, because the illness was dispersed by sailing ships, there were lengthy lapses of about 10-40 years between outbreaks (Gubler, 2006). Every year worldwide, millions of people have been suffering from DENV in the form of dengue hemorrhagic fever, dengue shock syndrome and general fever illness that eventually gives in fatal result in health and economy of whole country. Over the years various studies have been conducted to identify effective drug against DENV which could save thousands of lives in a year. Despite extensive research, there are no specific antiviral treatments for DENV, necessitating the exploration of novel therapeutic agents (Obi *et al.*, 2021). Dengvaxia, a live attenuated vaccine, is the WHO-approved vaccine for children (9 to 16 years) who have previous dengue infection (Pintado Silva *et al.*, 2023). However, its effectiveness is limited to individuals with a prior history of dengue infection, and its use in those without prior exposure may increase the risk of severe dengue. As a result, supportive care remains the mainstay of treatment, including transfusions for thrombocytopenia or bleeding, oral hydration, fluid administration, and antipyretics for fever management.

Flaviviridae family virus DENV is a single-stranded, positive-sense ribonucleic acid virus with a genome around 11 kilobases in size (Holmes and Burch, 2000). It is particularly noteworthy since it has four antigenically unique serotypes viz. DENV-1, DENV-2, DENV-3 and DENV-4 each of them has significant amount of genetic diversity. A systematic analysis of numerous publications revealed that DENV-2 is far more contagious than the other serotypes. DENV is composed of seven nonstructural proteins (NS1, NS2A, NS2B, NS3, NS4A, NS4B, and NS5) in addition to the three structural proteins capsid (C), membrane (M) which includes a membrane precursor (PrM), and envelope (E). The conformational variations of M and E proteins at varying ambient pH levels determine the infectious and noninfectious phases of mature and immature DENV (Halstead, 1989; Kuhn *et al.*, 2002; Perera and Kuhn, 2008). RNA triphosphate (RTPase) and nucleocapsid triphosphate (NTPase) activities are encoded by NS3 and NS2B protein is necessary cofactor for the apo-behaving NS3 protease. The proteolytic cleavage is carried out by NS2B and NS3 in viral replication cycle

(Wahaab *et al.*, 2021; Mukhtar and Khan, 2023). NS2B stabilizes the structure of NS3 and facilitates substrate binding, while NS3 possesses the protease activity responsible for cleaving the viral polyprotein into functional components necessary for viral replication (Yusof *et al.*, 2000).

With the advancement of technology and research, the phytochemicals from different plants such as *Carica papaya*, *Acacia catechu, Arrabidaea pulchra*, and *Curcuma longa* have been used in the treatment of DENV. Most studies investigate flavonoids, a class of phenolic compounds found in plants, as antivirals (Brandão *et al.*, 2013; Padilla-s *et al.*, 2014; Panya *et al.*, 2019; Norahmad *et al.*, 2019). Flavonoids exhibit powerful antioxidant properties, effectively neutralizing free radicals and exhibiting antiviral activity against various viruses, including DENV-2 and influenza A, chikungunya, and hepatitis B. Quercetin, a key flavonoid, further enhances this effect by modulating the NF-κB, IL-17, and Toll-like receptor signaling pathways, reducing cytokine release, alleviating inflammation, and regulating overactive immune responses (Zheng *et al.*, 2021).

Myricetin (MYR) is a flavonoid and chlorogenic acid (CGA) is a phenolic acid compound. MYR and CGA have antioxidant, anti-inflammatory, and antiviral properties, making them effective in combating oxidative stress, inflammation, and viral infections. The combined therapeutic potential highlights their role in managing various health conditions. CGA family members are dietary phenolic acid compounds found in plants, including quinic acid, caffeic acid, ferulic acid, and p-coumaric acid. The natural products show protective effects against cancer, viral and bacterial infections, chronic inflammatory and age-related disorders. Khanal *et al.* (2024) analyzed the inhibition potential of caffeic acid and p-coumaric acid against HDAC2 enzyme, Basnet *et al.* (2023) studied the inhibitory nature of natural products against human pancreatic alpha-amylase, Acharya *et al.* (2024) reported dolichin A having strong binding interactions with lactoferrin protein, and Gyawali *et al.* (2024) identified catechin as the main protease inhibitor of SARS-CoV-2 Omicron variant by using *in silico* techniques. CGA has limited bioavailability in plant foods due to cell wall esterification. Therapeutic potential, biological functions and toxicity assessment of CGA were well explained in previous research (Watanabe *et al.*, 2006; Faria *et al.*, 2020; and Gupta *et al.*, 2022). CGA is richly found in green coffee beans and fruit (apples, pears, and blueberries), vegetables (eggplants and potatoes). CGA has a good safety profile, no adverse effects, and is well-tolerated by humans. In an acute toxicity experiment, mice showed no side effects after two weeks of intake (Nguyen *et al.*, 2024). Various fruits viz. berries, grapes, and leafy vegetables, and teas contain MYR. MYR has similar structure as that of quercetin which is one of the important bioactive compounds showing antimicrobial properties. Only a difference is that MYR has an extra hydroxyl group in one of the aromatic rings, i.e. B-ring. The properties of MYR and CGA were explored alongside quercetin to expand the pool of potential drug candidates against the DENV virus. Their comparable antiviral effectiveness highlights their potential to work alongside quercetin in developing effective treatments. The structures of quercetin (PubChem CID: 5280343), MYR (PubChem CID: 5281672) and CGA (PubChem CID: 1794427) are shown in Figure 1. This study aims to evaluate the efficacy of MYR and CGA as potential drug candidates against DENV through *in silico* approaches. *In silico* methods are computational techniques used to predict molecular interactions, offering significant savings in time and resources. *In vitro* methods are used for experimental testing in a controlled laboratory setting to provide more direct biological relevance. The *in silico* methods predict results by analyzing receptor-ligand interactions, which must be validated through *in vitro* and *in vivo* studies to ensure effectiveness and suitability for clinical application.

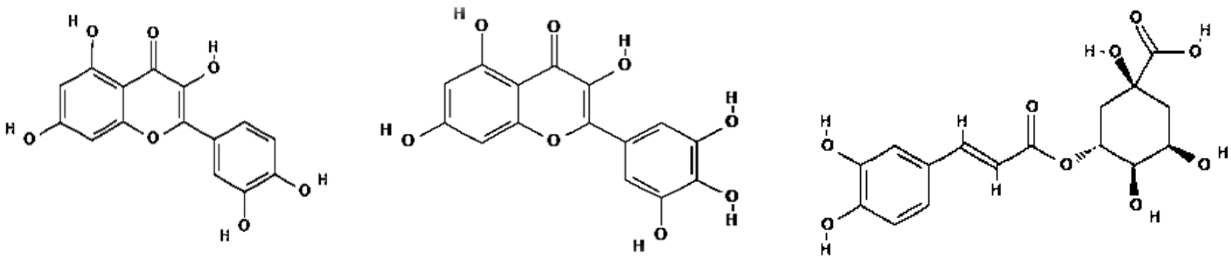

(a) (b) (c)

Figure 1. Structure of three phytochemicals (a) quercetin: $C_{15}H_{10}O_7$, (b) myricetin: $C_{15}H_{10}O_8$, and (c) chlorogenic acid: $C_{16}H_{18}O_9$

MATERIALS AND METHODS

The primary three-dimensional structure of two-chain NS2B/NS3 protease (PDB ID: 2FOM) was obtained from the protein data Bank website (http://www.rcsb.org) to get detailed view of the enzyme's spatial arrangement allowing accurate analysis of molecular interactions at the ligand binding site. Once the co-crystallized ligand fragments (glycerol and chloride) and water molecules were removed from the structure, the protein was saved in PDB format using

PyMOL software. The protein structure was further refined using SWISS-MODEL to fulfill the missing atoms or residues. The resulting protein structure was loaded in AutoDock Tools in order to perform molecular docking.

After refinement using SWISS-MODEL server, the NS3 (chain A) protease domain typically includes residues from the middle portion from 7 to 53 of the NS3 protein. Similarly, NS2B (chain B) protease is the hydrophilic portion that acts as a cofactor for the NS3 protease generally resembles from 18 to 167 residues. The amino acid residues of NS2B/NS3 protease (composition of chain A and chain B shown in Figure 2) were renumbered to correct an unexpected overlap during molecular docking and MD trajectory analyses (Figure 2). The improved protease, with 196 total residues, was used for docking and dynamics with phytocompounds, ensuring accurate results. As a result, chain A starts at residue ID 7 and ends to 53, whereas chain B starts at residue ID 54 and ends to 203. The process for docking and dynamics with the corresponding phytocompounds uses the improved protease, which has 196 residues overall.

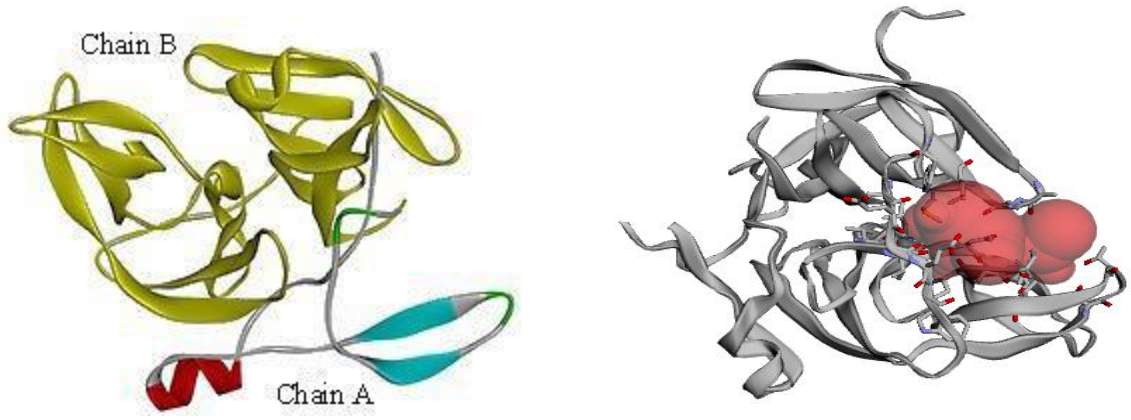

(a) (b)

Figure 2. (a) Structure of dengue virus NS2B/NS3 protease (2FOM.PDB) with two chains A and B consisting of 196 amino acid residues, (b) ligand binding pocket with highest surface area and cavity volume

The catalytic sites of the protein were identified using the CASTp online server (http://sts.bioe.uic.edu/castp/). The most viable binding cavity has pocket area of 301.43 $Å^2$ and pocket volume of 251.77 $Å^3$ of the protein (Tian *et al.*, 2018). The inbuilt AutoDock 4.2.6 Vina wizard in PyRx was used to screen ligands and evaluate the binding effectiveness of each one.

Molecular Docking

Docking studies were conducted to predict the binding affinity and orientation of the ligands within the active site of the protease. Especially when working with complex molecules like CGA, AutoDock is widely used for a grid-based approach to evaluate their docking poses. This study used AutoDock 4.2.6 (Morris *et al.,* 2009) to dock phytocompounds into active binding sites, with each receptor protein and ligand loaded into AutoDock Tools (Huey *et al.,* 2012). The receptor and ligand were saved in PDBQT formats, and grid parameters were selected for virtual screening. The grid dimensions were set to 70 × 70 × 70 Å along the X, Y, and Z axes respectively to ensure entire active biding sites were covered along with surrounding regions that eventually maximize the accuracy of ligand docking. The grid box was centered around X = -7.226, Y = -14.994, and Z = 5.444 Å and the grid point spacing was placed as 0.375 Å. The Lamarckian genetic algorithm generated docking parameters and log files, with the best-docked conformer saved in PDBQT format. The reduced grid might exclude parts of active binding site, potentially missing the key interactions critical for effective inhibitor binding. The docking results for the complexes with the highest binding energy and the strongest interactions were analyzed with Biovia Discovery Studio Visualizer. The best binding pose of the protein-ligand complex was subjected to MD simulations.

Molecular Dynamics Simulations

Molecular dynamics (MD) simulation is a powerful computational technique used to study the stability of a protein-ligand complex, accurately mimicking the conditions of both *in vitro* and *in vivo* experiments. *In vitro* methods check compounds in isolated cells to evaluate their biological effects, whereas *in vivo* methods assess a compound's efficacy, toxicity and therapeutic potential in whole organism. While docking identifies potential binding sites, MD simulations help understand how the complex behaves dynamically, assessing its stability, binding affinity, and conformational changes explained in the previous research (Lamichhane *et al.,* 2021; Maharjan *et al.,* 2024; Chhetri *et al.,* 2024). All the MD simulations were performed using GROningen MAChine for Chemical Simulations (GROMACS) version 2019.6 (Van Der Spoel *et al.*, 2005) and using CHARMM 36 force field (Huang and MacKerell Jr., 2005). The CHARMM compatible force field parameters

of the ligands were obtained from SwissParam server (Zoete *et al.*, 2011). The MD simulations of the selected protein-ligand complexes were performed by setting the time-step of 2 fs/step at TIP3P water solvent (dodecahedron box neutralized with Na^+ and Cl^- ions) at a constant temperature of 300 K. The NVT and NPT run were performed for 100 ps each, and the NPT production run was performed for 100 ns using the time interval of 100 ps between the frames to generate the MD trajectories consisting of 1000 frames. Here's an overview of the typical steps involved in conducting an MD simulation. The physical parameters such as root mean square deviation (RMSD), root mean square fluctuation (RMSF), radius of gyration (R_g), hydrogen bonding, and solvent accessible surface area (SASA) were examined to check the stability, conformational changes, and binding efficacy of the protein-ligand complexes. The end-state binding free energy, i.e. molecular mechanics generalized Born surface area (MM/GBSA) calculations were performed by using gmx_MMPBSA tools (Valdés-Tresanco *et al.*, 2021) from the GROMACS MD trajectories of the protein-ligand system.

ADMET Predictions

A drug candidate may reach its target in the body at a high enough concentration and remain there in a bioactive state for the anticipated biologic activities to take place for it to be successful as a medication. ADMET (absorption, distribution, metabolism, excretion, and toxicity) properties are crucial for assessing the safety and efficacy of phytocompounds and their derivatives including CGA and MYR in treatment. These compounds must exhibit good pharmacokinetics and low toxicity while adhering to Lipinski's Rule of Five for optimal drug-like behavior. By using SwissADME web tool (Daina *et al.*, 2017), the pharmacokinetic parameters, ADME properties, and drug-likeness features were identified. Furthermore, admetSAR (Cheng *et al.*, 2012) and the ProTox II (Banerjee *et al.*, 2018) web tools were used to forecast toxicity.

RESULTS AND DISCUSSION

Molecular Docking

At the active site of NS2B/NS3 main protease, different types of interactions take place involving H-bonds. Lesser the value of binding energy, interactions and bonds between the protein and ligands, molecules will be more stable and stronger. In molecular docking, binding energy describes how strongly a protein interacts with a ligand. Numerous elements, including patterns of hydrogen bonds and hydrophobic interactions, have an impact on it.

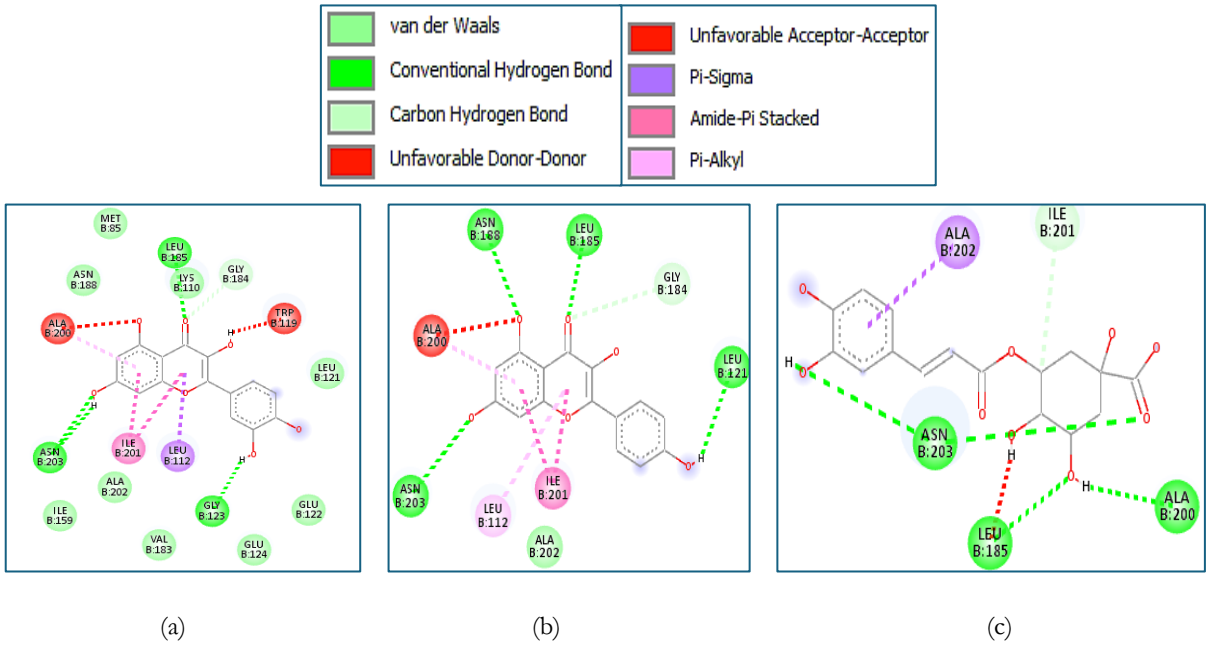

(a) (b) (c)

Figure 3. Two-dimensional interaction diagrams for the best docked poses of (a) quercetin, (b) myricetin and (c) chlorogenic acid in complex with NS2B/NS3 main protease using Biovia Discovery Studio Visualizer.

Quercetin is one of the important bioactive compounds showing antimicrobial, anticancer, antioxidant and antidiabetic properties (Shabir *et al.*, 2022; Azeem *et al.*, 2023). Its binding energy is -7.9 kcal/mol with NS2B/NS3 protease ensuring strong interactions. Likewise, four H-bonds, one pi-sigma, one pi-alkyl and two amide pi-stacked bonds have been formed at the active binding site of the main protease as shown in Figure 3-a. Quercetin facilitates the conventional H-bonds with ASN203, GLY123 and LEU185. It interacts with ALA200 by unfavorable acceptor-acceptor as well as pi-alkyl bond and with TRP119 through unfavorable donor-donor bond. Furthermore, quercetin interacts with LEU112, ILE201 and ALA202 forming pi-sigma

bond, amide-pi stacked bond, and van der Waals interaction respectively. In this way, MYR and CGA also perform strong interactions with the active site residues as shown in the 2D diagrams (Figure 3- b, c). The binding energy of MYR and CGA are -7.9 and -7.1 kcal/mol with the NS2B/NS3 protease respectively. MYR interacts with the active residues forming five conventional H-bonds, two amide-pi-stacked, and one for pi-sigma, unfavorable donor-donor, carbon H-bond and unfavorable acceptor-acceptor interactions respectively. It forms conventional H-bonds with ASN203, GLY123, and LEU185. Similarly, two amide-pi stacked bond with ILE201 and one pi-sigma with LEU112, one van der Waals with ALA202, one carbon H-bond with GLY184, one pi-sigma with LEU112 are formed. It also interacts with ALA200 with unfavorable acceptor-acceptor bond and forms unfavorable donor-donor bond with TRP119. Likewise, CGA facilitates four conventional H-bonds, two with ASN203, one with LEU185, and one with ALA200. It also forms one carbon H-bond with ILE201 and one pi-sigma bond with ALA202. These interactions and bond facilities in the respective structure including CGA and MYR improve their binding stability and affinity with the target protein, supporting their role as the strong inhibitors.

Molecular Dynamics Simulations

The phytochemicals such as quercetin, MYR and CGA in complex with NS2B/NS3 main protease have been selected for MD simulations based on their docking scores, size of the molecules, medicinal background, biochemical and ADMET properties. There is limited research on MYR and CGA analyzing the results from MD trajectory analysis compared with quercetin. Each of the three compounds appears to be stable in 100 ns MD simulations as identified from RMSD, RMSF, R_g, H-bonding, SASA and end-point free energy (MM/GBSA) calculations.

Table 1. Mean±SD of the parameters observed from the trajectories of NS2B/NS3 main protease in complex with the phytochemicals during 100 ns MD simulations

Protein in complex with	Average No. of H-bonds	Protein Rg (nm)	Residue RMSF (nm)	Protein RMSD (nm)	Ligand RMSD (nm)	Protein SASA (nm^2)
Quercetin	2.4 ± 1.3	1.73 ± 0.03	0.22 ± 0.21	0.45 ± 0.09	0.09 ± 0.02	115.54 ± 3.53
Myricetin (MYR)	2.7 ± 1.2	1.71 ± 0.02	0.18 ± 0.16	0.30 ± 0.78	0.05 ± 0.03	114.94 ± 3.66
Chlorogenic acid (CGA)	2.4 ± 1.4	1.71 ± 0.02	0.17 ± 0.14	0.26 ± 0.05	0.19 ± 0.02	121.48 ± 3.03

RMSD

RMSD is used to understand conformational changes and the stability of the protein-ligand complex. The reduced RMSD values signify more stability and fewer conformational changes.

Figure 4 details the RMSD variations for protein and ligand in their respective complexes. When the protease is in complex with three distinct ligands quercetin, MYR and CGA, the average RMSD values for the NS2B/NS3 protein in complex with the ligands quercetin, MYR and CGA are 0.45 ± 0.09, 0.30 ± 0.78, and 0.26 ± 0.05 nm, respectively which are depicted in Table 1. Likewise, the average RMSD values for each of the three ligands are 0.09 ± 0.02, 0.05 ± 0.03, and 0.19 ± 0.02 nm, respectively. An average RMSD value of less than 0.3 nm is the reference limit for the better stability of the system.

RMSF

RMSF represents residue-wise atomic fluctuations at the C_α-backbone of the protein, providing crucial insights into the dynamical behavior related to structural flexibility and stability of the NS2B/NS3 protease. Average RMSF values for the C_α-backbone of protease in complexes with quercetin, MYR and CGA are 0.22 ± 0.20, 0.18 ± 0.16, and 0.17 ± 0.14 nm, respectively. The lower RMSF values of the residues in complex with MYR and CGA compared to quercetin indicate greater stability and reduced flexibility of the complexes, highlighting MYR and CGA as potentially stronger inhibitors.

The RMSF values of the respective amino acids in the complexes are quite similar showing stable and constrained regions giving lower values. The residues between IDs 26 to 58 show the higher fluctuations (Figure 5) which is due to the free loop regions of chain A and chain B. In the NS2B/NS3 protease, chain A is isolated from the heterodimer structure that increases more oscillation of that part during simulation time frame.

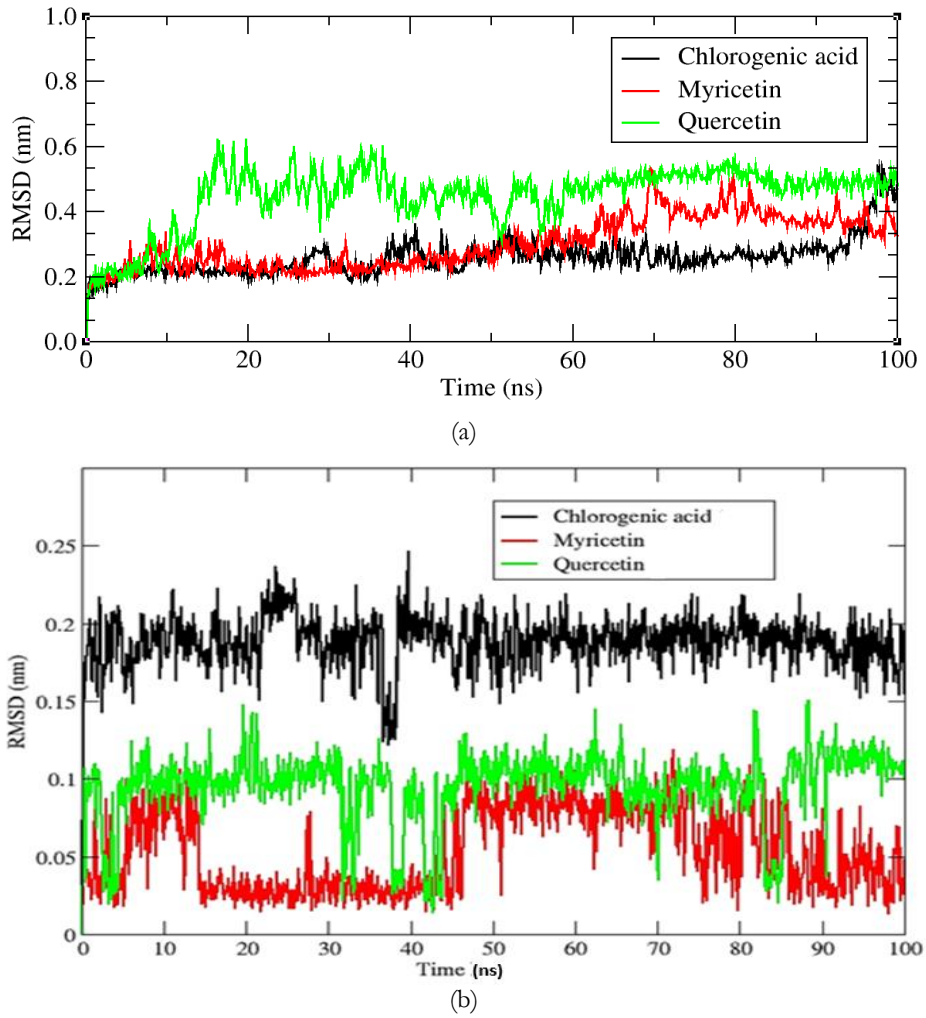

Figure 4. Variation in RMSD of (a) NS2B/NS3 protease in complex with ligands and (b) phytocompounds quercetin, myricetin and chlorogenic acid

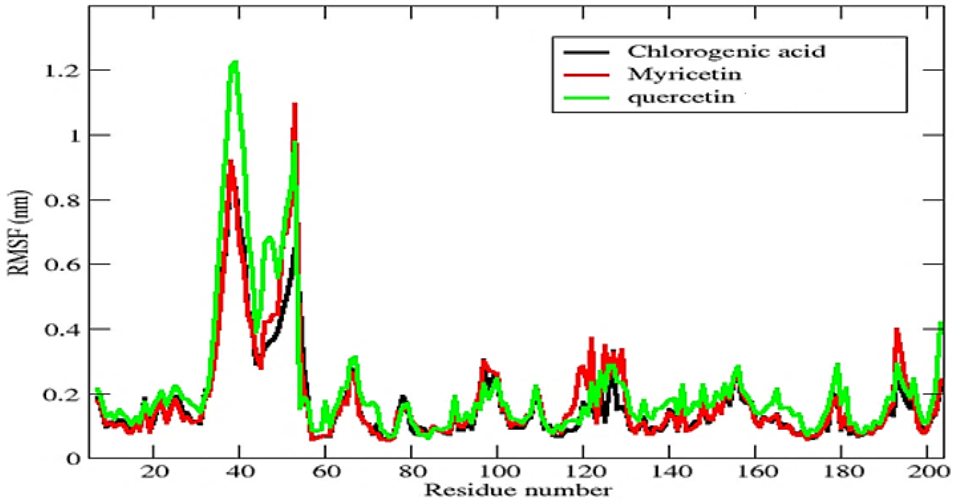

Figure 5. RMSF of the protein backbone in complex with quercetin, myricetin and chlorogenic acid during 100 ns MD simulations

Radius of Gyration

The structural compactness and conformational stability of the protein-ligand complex is explored by the parameter R_g. During 100 ns MD simulations, the R_g values of NS2B/NS3 main protease in complex with quercetin, MYR and CGA are 1.73 ± 0.03, 1.71 ± 0.02, and 1.71 ± 0.02 nm, respectively. The variations in R_g of the protein systems have been shown in Figure 6.

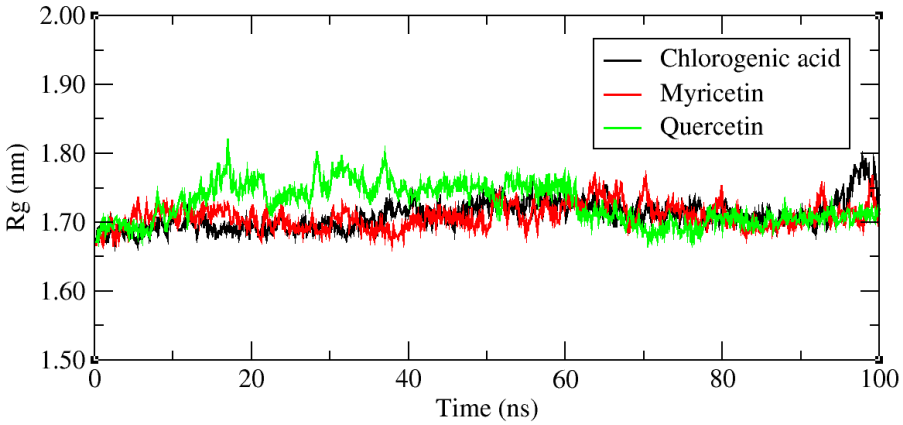

Figure 6. Changing radius of gyration of NS2B/NS3 protease in complex with quercetin, myricetin and chlorogenic acid during 100 ns simulations

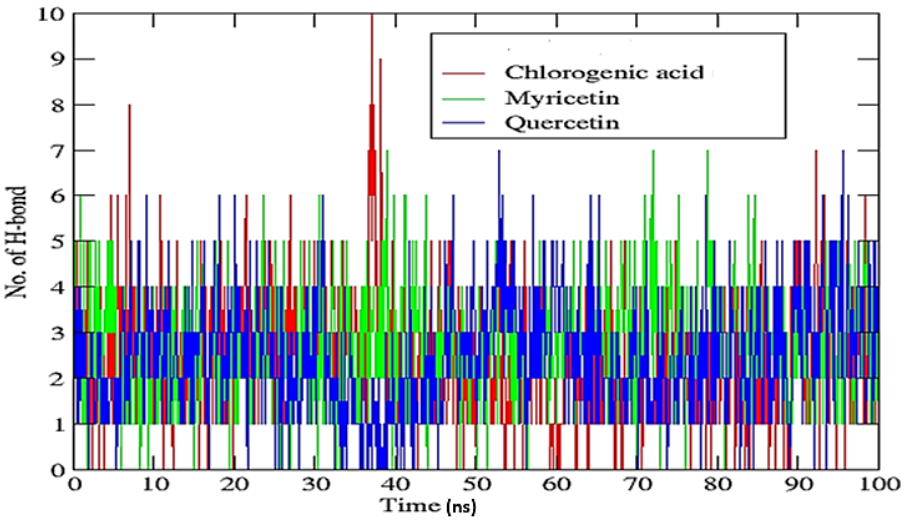

Figure 7. Variations number of H-bonds between NS2B/NS3 protease and ligands quercetin, myricetin and chlorogenic acid during 100 ns MD simulations

MYR has the least R_g compared to both, and it also gives more stable values providing insight into the structural compactness and conformational stability of the protein-ligand complex. The complex with quercetin seems to fluctuate more at the beginning of the simulation due to unstable energy state, and it shows higher R_g indicating flexible nature during the simulation time frame. Likewise, the complex with CGA shows high fluctuation at the last despite quite low R_g values at the beginning of the simulation. The larger fluctuations seen in the graphs should be due to the heterodimer NS2B/NS3 main protease chains vibrating independently during MD simulations, however, the measured deviations in the physical parameters are in the acceptable range.

H-Bonding

The average number of H-bonds formed between NS2B/NS3 main protease and the ligands quercetin, MYR and CGA are 2.4 ± 1.3, 2.7 ± 1.2, and 2.4 ± 1.4, respectively during 100 ns MD simulations. Here, MYR shows better binding with its receptor protein. The H-bond distributions are shown in Figure 7.

SASA

Intermolecular interactions involving hydrophobic native contact inside the protein have a significant impact on the inhibition of the enzyme. As a result, to calculate the contribution of hydrophobic and hydrophilic residues to the solvent molecules

throughout the simulation, it is also required to ascertain the SASA of the complex.

The variation of SASA during the simulation time frames are shown in Figure 8. The mean±SD values are 115.54 $\pm$ 3.53, 114.94 $\pm$ 3.66, and 121.48 $\pm$ 3.03 nm^2 for the protein complexes with quercetin, MYR and CGA respectively. CGA shows more fluctuation in H-bonding while MYR exhibits less fluctuation. The MYR bound protein has comparatively lower and stable SASA throughout the simulation. Hence, MYR possesses greater compactness and stability with the NS2B/NS3 protease.

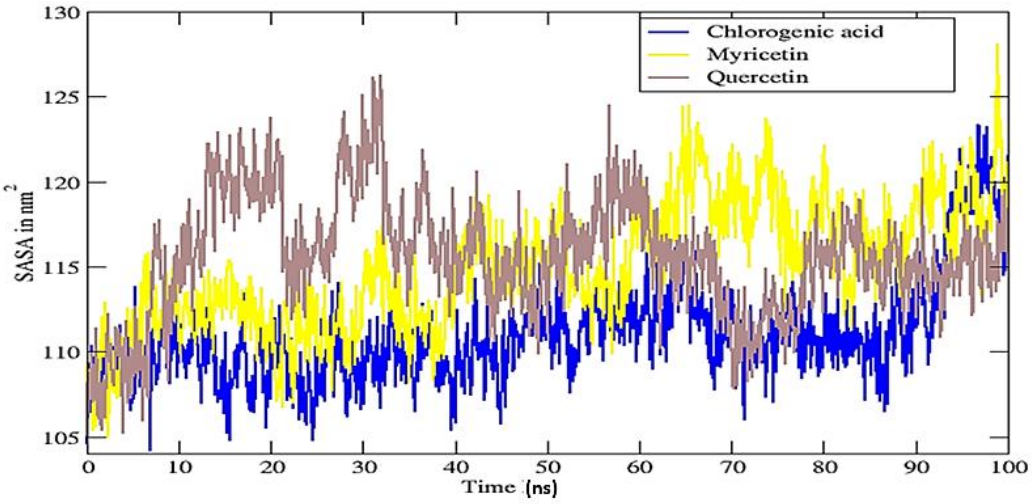

Figure 8. Variations of SASA of the protein systems with quercetin, myricetin and chlorogenic acid during their MD simulations

MM/GBSA Calculations

The energetic components (electrostatic, van der Waals and solvation energy) giving rise to the total MM/GBSA free energy of quercetin, MYR and CGA in complex with NS2B/NS3 main protease of dengue virus analyzed from the last 20 ns equilibrating frames of the MD trajectories have been presented in Table 2 and demonstrated by bar diagrams in Figure 9.

Table 2. Average contributions of energetic components to the net binding energy of selected compounds against NS2B/NS3 protease obtained by MM/GBSA calculations

Compounds	Gaseous Energy (kcal/mol)		Solvation Energy (kcal/mol)		Grand Total (kcal/mol)		
	VDWAALS	EEL	EGB	ESURF	GGAS (VDWAALS+EEL)	GSOLV (EGB+ESURF)	TOTAL
Quercetin	-31.92±3.44	-22.85±6.91	35.62±4.01	-4.54±0.25	-54.77±6.45	31.08±4.53	-23.69±3.09
Myricetin (MYR)	-31.59±3.11	-35.40±5.95	46.23±4.05	-4.30±0.22	-66.98±6.01	41.93±4.00	-25.05±3.19
Chlorogenic acid (CGA)	-31.87±2.74	-24.94±7.73	41.41±5.49	-4.82±0.34	-56.81±7.57	36.59±5.31	-20.22±3.02

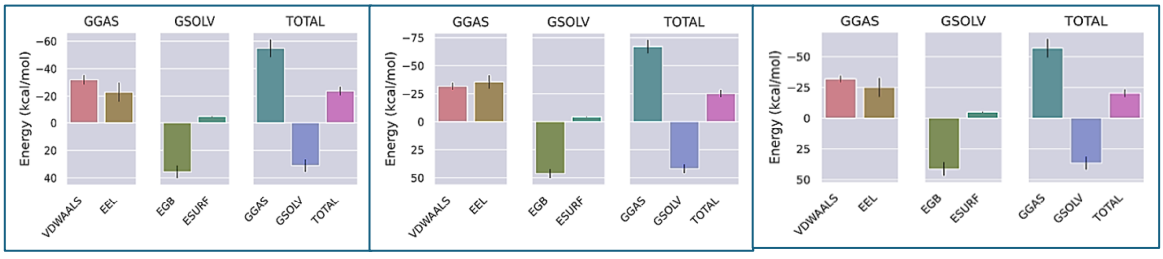

(a) (b) (c)

Figure 9. Average contribution of energetic components to the binding energy of (a) quercetin, (b) myricetin and (c) chlorogenic acid in NS2B/NS3 main protease of dengue virus

Taking the stable conformers of the last 20 ns MD simulations, each of the three protein-ligand complexes exhibits stable binding free energy. The mean±SD values are -23.69±3.09, -25.05±3.19, and -20.22±3.02 kcal/mol for the complexes with quercetin, MYR and CGA, respectively. The main protease in complex with MYR has the lowest free energy. Hence, it is energetically favorable complex than others. Although MM/GBSA

free energy of binding of each ligand lies within the same error limit, the main protease in complex with quercetin and MYR exhibits considerably better end-point free energy than CGA over the course of simulation. These results are also comparable with the end-state MM/GBSA free energy values of the natural products reported on the recent literature; for example, catechin has -20.5±2.5 kcal/mol with SARS-CoV-2 Omicron Mpro (Gyawali *et al.*, 2024), caffeic acid has -16.32±2.62 kcal/mol with HDAC2 enzyme (Khanal *et al.*, 2024) and dolichin-A has -17.61±4.03 kcal/mol with lactoferrin (Acharya *et al.*, 2024).

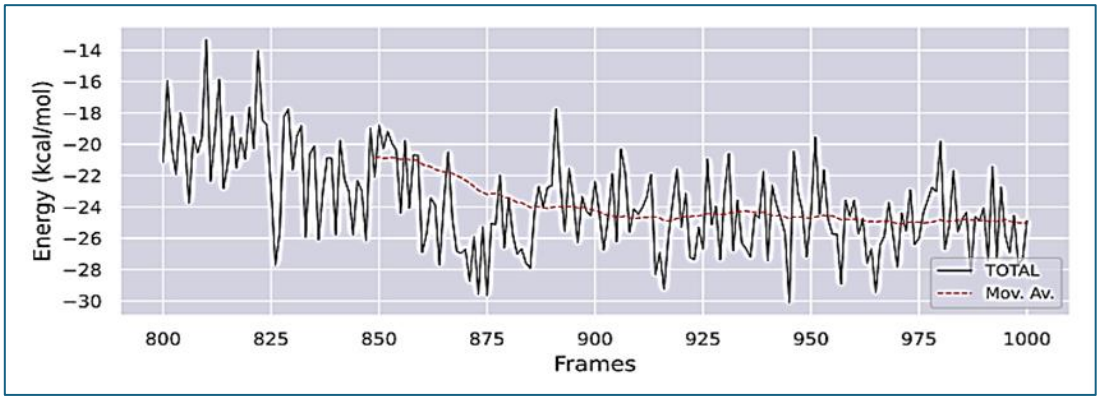

(a)

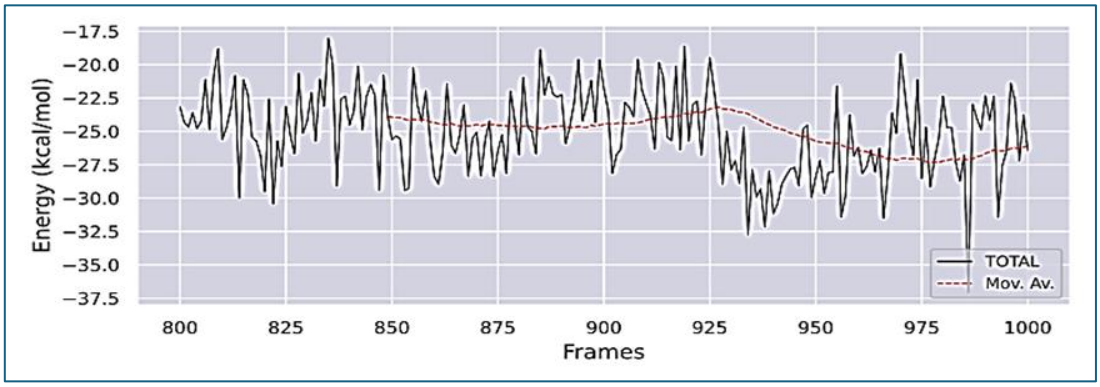

(b)

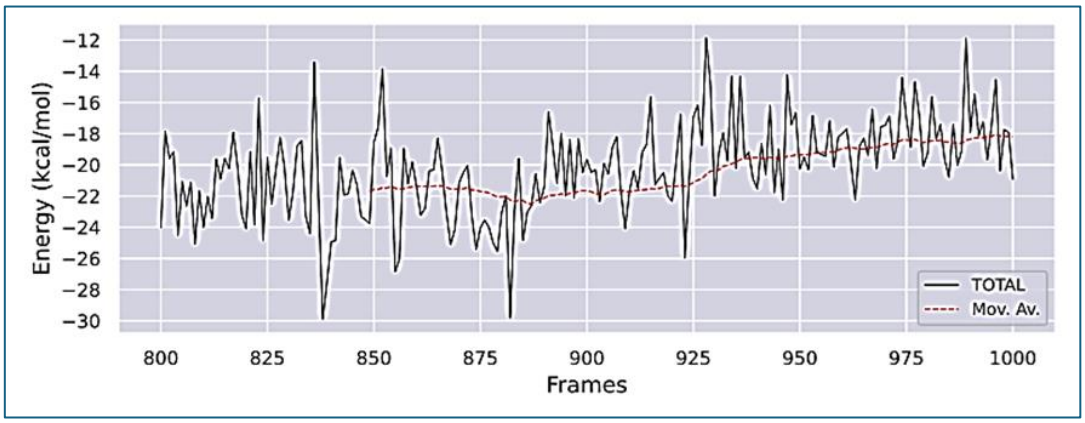

(c)

Figure 10. Fluctuating total MM/GBSA free energy of (a) quercetin, (b) myricetin and (c) chlorogenic acid in NS2B/NS3 main protease during the course of the last 20 ns stable frames taken from 100 ns MD trajectories

The fluctuating total free energy of binding lies in the large negative region in every frame (Figure 10) which explains that the proposed compounds bind properly to the dengue virus protease during the course of simulations. Figure 11 describes the contribution of respective residues in the protease ligand complex over

the simulation time. Here, GLY184, LEU185, ILE201 and ALA202 are the common residues of chain B contributing to the binding of all ligands quercetin, MYR and CGA significantly as shown by the heat maps (Figure 12).

Overall, MYR gets better binding scores and performs good stability inhibiting NS2B/NS3 main protease and acting as a potential drug candidate against dengue.

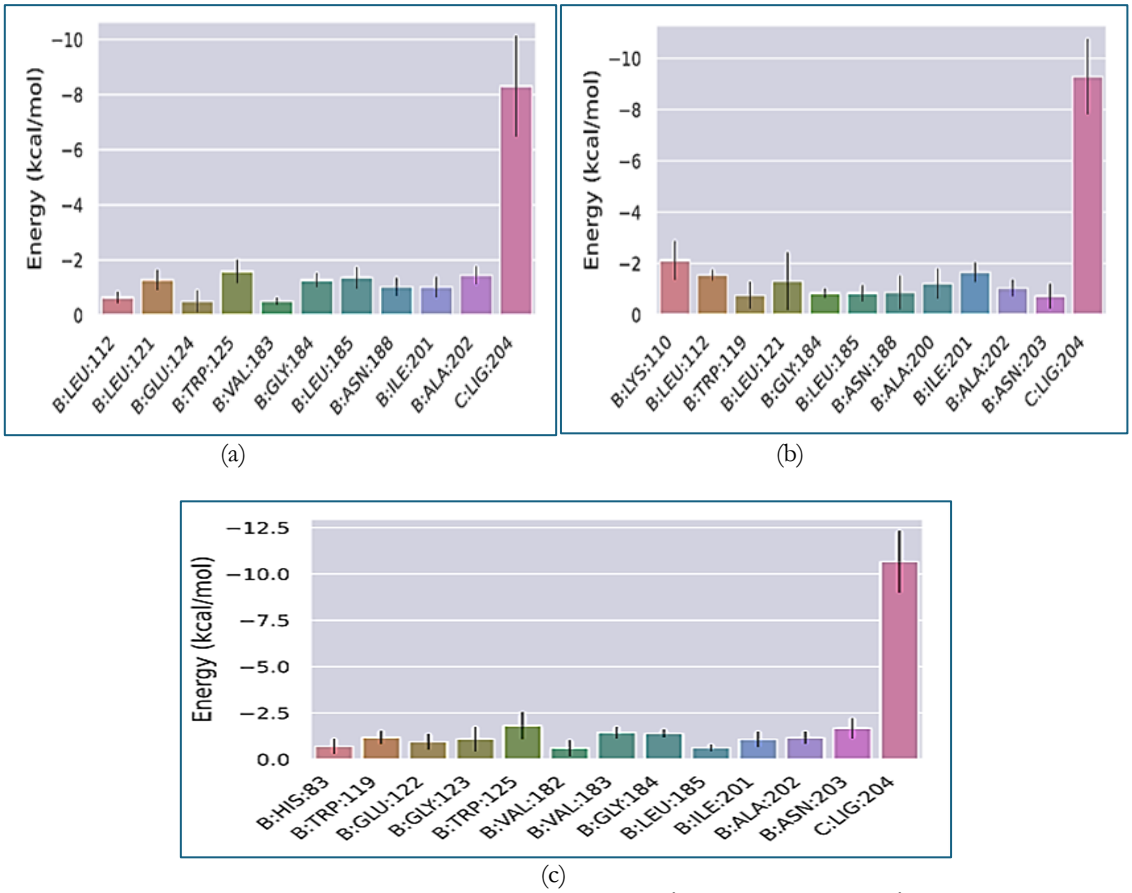

Figure 11. Contributions of active residues (cut-off energy of -0.5 kcal/mol) to the total MM/GBSA binding free energy of (a) quercetin, (b) myricetin and (c) chlorogenic acid to the dengue virus NS2B/NS3 main protease

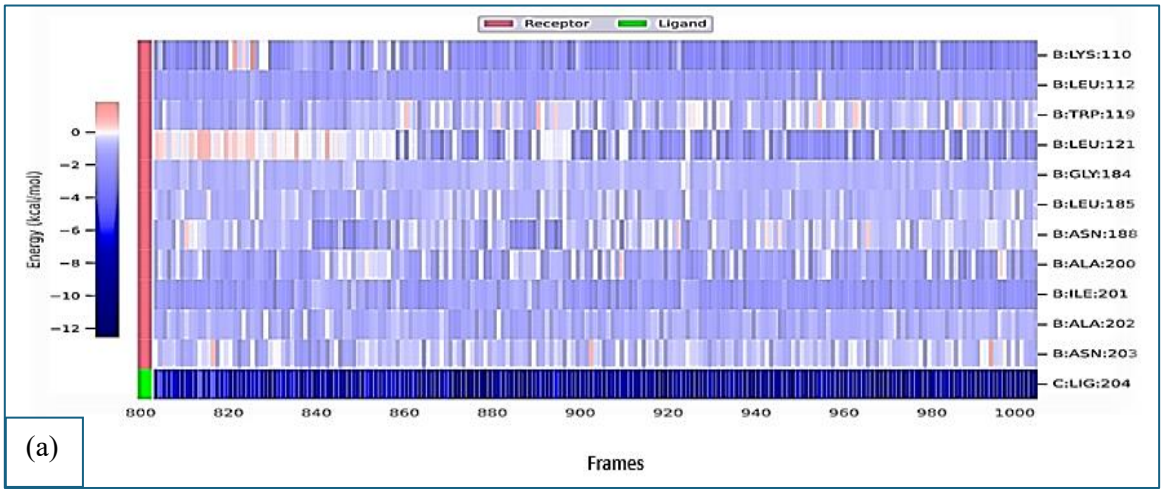

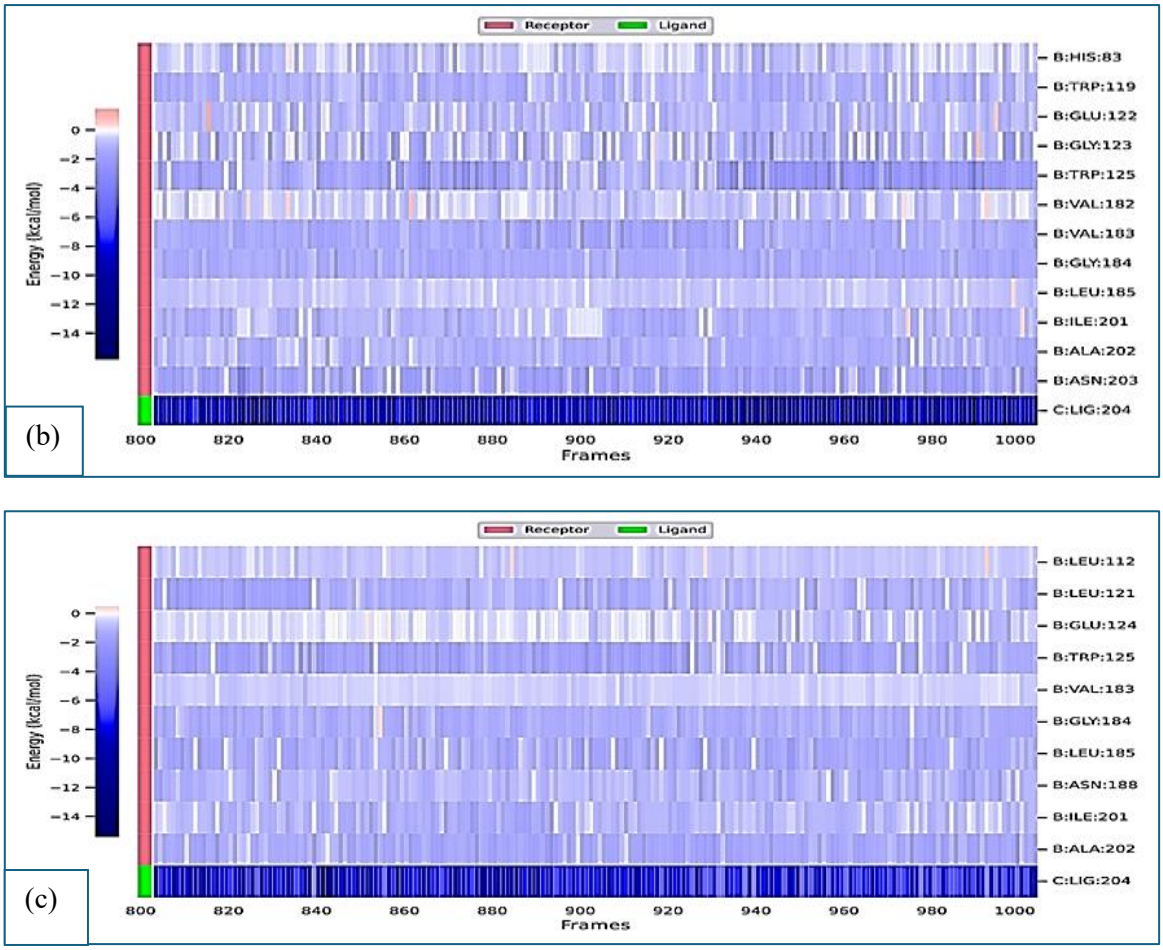

Figure 12. Fame wise contributions of the active residues (cut-off energy of -0.5 kcal/mol) to MM/GBSA binding free energy of (a) quercetin, (b) myricetin and (c) chlorogenic acid to the dengue virus NS2B/NS3 main protease during the last 20 ns of equilibrating MD simulations

ADMET Analysis

SwissADME results show that quercetin, MYR and CGA have the $\log K_p$ values of -7.05 cm/s, -7.40 cm/s and -8.76 cm/s indicating lower skin permeability. Quercetin has high GI absorption, while MYR and CGA have low GI absorption. CGA has lower bioavailability score of 0.11 than the other contenders which mostly have a bioavailability value of 0.55. The predicted water solubility (log *S* value) of the proposed compounds ranges from -1.62 to -3.91 that suggests moderately water-soluble.

Lipinski's rule of five is a guideline in drug design that helps assess a compound's potential to become an orally active drug (Lipinski *et al.,* 2012). It states that for optimal oral bioavailability, a compound should have molecular weight less than 500 Daltons, LogP (partition coefficient) less than 5, no more than 5 hydrogen bond donors, no more than 10 hydrogen bond acceptors. In drug discovery, lead compounds are initial candidate molecules with desirable biological activity against a target. Quercetin has zero violation showing very good drug-likeness score, however, MYR and CGA show 1 violation of Lipinski's rule of five. From the BOILED Egg analysis (Figure 13), quercetin is well absorbed by GI track whereas MYR and CGA have low GI absorption. The radar diagram (Figure 14) shows that quercetin and MYR have slightly higher insaturation than the normal range whereas CGA has its normal value. MYR and CGA have slightly higher TPSA (total polar surface area) than the normal range.

Compounds with lower predicted LD50 values may exhibit higher potency but also carry greater risks of toxicity. Class 1 shows deadly if ingested ($LD50 \leq 5$ mg/kg). In this way, the dangerous limits of doses for class 2, 3, 4, 5 and 6 are ($5 < LD50 \leq 50$), ($50 < LD50 \leq 300$), ($300 < LD50 \leq 2000$), ($2000 < LD50 \leq 5000$), and ($LD50 > 5000$), respectively, all measured in mg/kg (Banerjee *et al*., 2018). Here, the drug candidates falling in the category of 5 and 6 classes appear to be safer than others. ProTox-II web server predicts that quercetin and MYR both have the same LD50 of 159 mg/kg falling on the class 3, and CGA has LD50 of 5000 mg/kg falling in the class 5 appearing less toxic in nature. Overall, except violating very few ADMET parameters, quercetin, MYR and CGA could be the good drug candidates against the dengue infection.

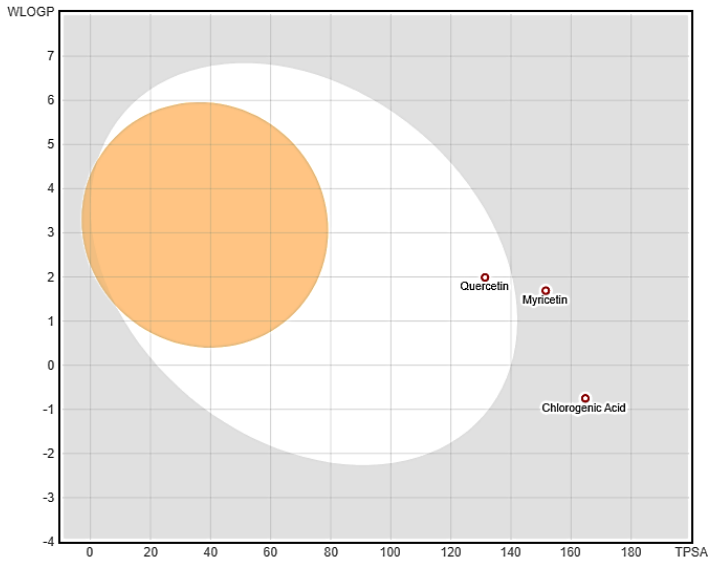

Figure 13. BOILED Egg analysis of the three drug candidates quercetin, myricetin and chlorogenic acid. The candidates falling in the yolk region are predicted to passively permeate BBB, falling in the white region can pass through GI track, and the red dots indicate that they are predicted not to be effluated from the central nervous system by the P-glycoprotein

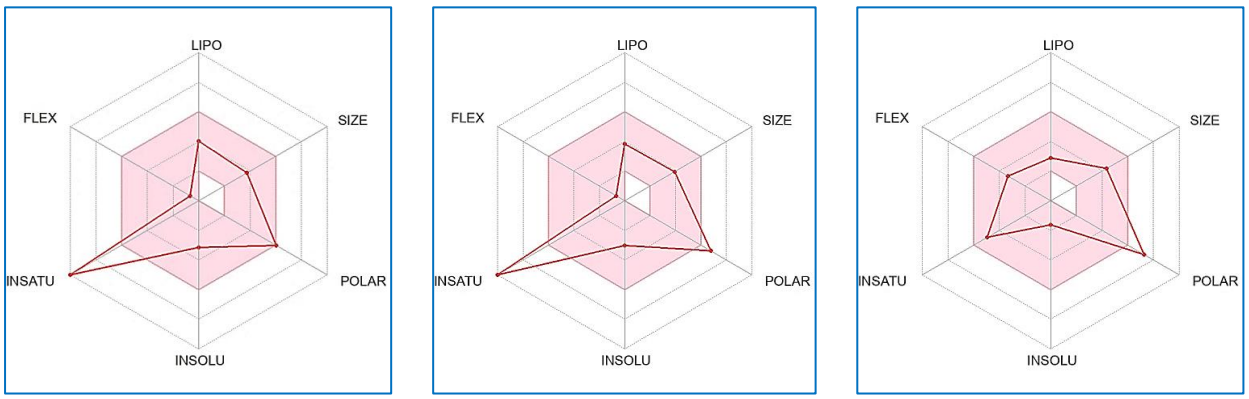

(a) (b) (c)

Figure 14. Radar diagram showing ADME properties of (a) quercetin, (b) myricetin and (c) chlorogenic acid. The colored zone is the suitable region for oral bioavailability defined by the ranges in SwissADME web tool; LIPO (lipophilicity): −0.7 < XLOGP3 < +5.0, SIZE: 150 < MW < 500 g/mol, POLAR (polarity): 20 < TPSA < 130 Å^2, INSOL (insolubility): -6 < log *S* < 0, INSATU (insaturation): 0.25 < Fraction Csp3 < 1, FLEX (flexibility): 0 < rotatable bonds < 9

CONCLUSIONS

The phytocompounds such as myricetin (MYR) and chlorogenic acid (CGA) bind properly to the active site of NS2B/NS3 main protease as identified from molecular docking, MD trajectory analysis, and end-state free energy calculations. In addition to quercetin, MYR and CGA result in compact stability at the main protease active site by analyzing RMSD, RMSF, R_g, H-bonding, and SASA. The MM/GBSA free energies of MYR and CGA in complex with dengue virus NS2B/NS3 main protease are found to be -25.05±3.19 kcal/mol and -20.22±3.02 kcal/mol. Therefore, MYR and CGA with good ADMET properties are identified as the potential drug candidates against dengue virus. However, further experimental verifications are required to know their effectiveness.

ACKNOWLEDGEMENTS

We acknowledge Nepal Academy of Science and Technology (NAST) for providing the Research Grant 2080/081 to the corresponding author.

AUTHOR CONTRIBUTIONS

Both authors have contributed equally to this research paper.

CONFLICT OF INTEREST

Authors declare that there is no conflict of interest.

DATA AVAILABILITY

The data that support the findings of this study are available from the corresponding author, upon reasonable request.

REFERENCES

Acharya, A., Khanal, M., Maharjan, R., Gyawali, K., Luitel, B.R., Adhikari, R., Mulmi, D.D., Lamichhane T.R. & Lamichhane, H.P. (2024). Quantum chemical calculations on calcium oxalate and dolichin A and their binding efficacy to lactoferrin: An in silico study using DFT, molecular docking, and molecular dynamics simulations. *AIMS Biophysics*, *11*(2), 142-165. https://doi.org/10.3934/biophy.2024010.

Azeem, M., Hanif, M., Mahmood, K., Ameer, N., Chughtai, F.R.S., & Abid, U. (2023). An insight into anticancer, antioxidant, antimicrobial, antidiabetic and anti-inflammatory effects of quercetin: A review. *Polymer Bulletin*, *80*(1), 241-262. https://doi.org/10.1007/s00289-022-04091-8.

Banerjee, P., Eckert, A.O., Schrey, A.K., & Preissner, R. (2018). ProTox-II: a webserver for the prediction of toxicity of chemicals. *Nucleic acids research*, *46*(W1), W257-W263. https://doi.org/10.1093/nar/gky318.

Basnet, S., Ghimire, M.P., Lamichhane, T.R., Adhikari, R., & Adhikari, A. (2023). Identification of potential human pancreatic α-amylase inhibitors from natural products by molecular docking, MM/GBSA calculations, MD simulations, and ADMET analysis. *Plos one*, *18*(3), e0275765. https://doi.org/10.1371/journal.pone.0275765.

Berman, H.M., Westbrook, J., Feng, Z., Gilliland, G., Bhat, T.N., Weissig, H., ... & Bourne, P.E. (2000). The protein data bank. *Nucleic Acids Research*, *28*(1), 235-242. https://doi.org/10.1093/nar/28.1.235.

Brandão, G.C., Kroon, E.G., Souza, D.E., Filho, J.D.S., & Oliveira, A.B. (2013). Chemistry and antiviral activity of Arrabidaea pulchra (Bignoniaceae). *Molecules*, *18*(8), 9919-9932. https://doi.org/10.3390/molecules18089919.

Cheng, F., Li, W., Zhou, Y., Shen, J., Wu, Z., Liu, G., ... & Tang, Y. (2012). admetSAR: a comprehensive source and free tool for assessment of chemical ADMET properties. *Journal of Chemical Information and Modeling*, *52*(11), 3099-3105. https://doi.org/10.1021/ci300367a.

Chhetri, S.P., Bhandari, V.S., Maharjan, R., & Lamichhane, T.R. (2024). Identification of lead inhibitors for 3CLpro of SARS-CoV-2 target using machine learning based virtual screening, ADMET analysis, molecular docking and molecular dynamics simulations. *RSC Advances*, *14*(40), 29683-29692. https://doi.org/10.1039/D4RA04502E.

Daina, A., Michielin, O., & Zoete, V. (2017). SwissADME: a free web tool to evaluate pharmacokinetics, drug-likeness and medicinal chemistry friendliness of small molecules. *Scientific reports*, *7*(1), 42717. https://doi.org/10.1038/srep42717.

Du, X., Li, Y., Xia, Y.L., Ai, S.M., Liang, J., Sang, P., ... & Liu, S.Q. (2016). Insights into protein–ligand interactions: mechanisms, models, and methods. *International Journal of Molecular Sciences*, *17*(2), 144.

Erbel, P., Schiering, N., D'Arcy, A., Renatus, M., Kroemer, M., Lim, S.P., ... & Hommel, U. (2006). Structural basis for the activation of flaviviral NS3 proteases from dengue and West Nile virus. *Nature Structural & Molecular Biology*, *13*(4), 372-373. https://doi.org/10.1038/nsmb1073.

Faria, W.C.S., da Silva, A.A., Veggi, N., Kawashita, N.H., de França Lemes, S.A., de Barros, W.M., ... & Bragagnolo, N. (2020). Acute and subacute oral toxicity assessment of dry encapsulated and non-encapsulated green coffee fruit extracts. *Journal of Food and Drug Analysis*, *28*(2), 337. https://doi.org/10.38212/2224-6614.1067.

Genheden, S., & Ryde, U. (2015). The MM/PBSA and MM/GBSA methods to estimate ligand-binding affinities. *Expert Opinion on Drug Discovery*, *10*(5), 449-461. https://doi.org/10.1517/17460441.2015.1032936.

Gubler, D.J. (2006). Dengue/dengue haemorrhagic fever: history and current status. In *New treatment strategies for dengue and other flaviviral diseases: novartis foundation symposium 277* (pp. 3-22). Chichester, UK: John Wiley & Sons, Ltd. https://doi.org/10.1002/0470058005.ch2.

Gupta, A., Atanasov, A.G., Li, Y., Kumar, N., & Bishayee, A. (2022). Chlorogenic acid for cancer prevention and therapy: Current status on efficacy and mechanisms of action. *Pharmacological Research*, *186*, 106505. https://doi.org/10.1016/j.phrs.2022.106505.

Gyawali, K., Maharjan, R., Acharya, A., Khanal, M., Ghimire, M.P., & Lamichhane, T.R. (2024). Identification of catechin as main protease inhibitor of SARS-CoV-2 Omicron variant using molecular docking, molecular dynamics, PCA, DCCM, MM/GBSA and ADMET profiling. *Natural Product Research*, 1-8. https://doi.org/10.1080/14786419.2024.2421907.

Halstead, S.B. (1989). Antibody, macrophages, dengue virus infection, shock, and hemorrhage: a pathogenetic cascade. *Reviews of Infectious Diseases*, *11*(Supplement_4), S830-S839. https://doi.org/10.1093/clinids/11.Supplement_4.S830.

Holmes, E.C., & Burch, S.S. (2000). The causes and consequences of genetic variation in dengue virus. *Trends in microbiology*, *8*(2), 74-77. https://doi.org/10.1016/S0966-842X(99)01669-8.

Huang, J., & MacKerell Jr, A.D. (2013). CHARMM36 all-atom additive protein force field: Validation based on comparison to NMR data. *Journal of Computational Chemistry*, *34*(25), 2135-2145. https://doi.org/10.1002/jcc.23354.

Huey, R., Morris, G.M., & Forli, S. (2012). Using AutoDock 4 and AutoDock vina with AutoDockTools: a tutorial. *The Scripps Research Institute Molecular Graphics Laboratory*, *10550*(92037), 1000.

Khanal, M., Acharya, A., Maharjan, R., Gyawali, K., Adhikari, R., Mulmi, D.D., Lamichhane T.R. & Lamichhane, H.P. (2024). Identification of potent inhibitors of HDAC2 from herbal products for the treatment of colon cancer: Molecular docking, molecular dynamics simulation, MM/GBSA calculations, DFT studies, and pharmacokinetic analysis. *PloS one*, *19*(7), e0307501. https://doi.org/10.1371/journal.pone.0307501.

Kuhn, R.J., Zhang, W., Rossmann, M.G., Pletnev, S.V., Corver, J., Lenches, E., ... & Strauss, J.H. (2002). Structure of dengue virus: implications for flavivirus organization, maturation, and fusion. *Cell*, *108*(5), 717-725. https://doi.org/10.1016/S0092-8674(02)00660-8.

Lamichhane, T.R., & Ghimire, M.P. (2021). Evaluation of SARS-CoV-2 main protease and inhibitor interactions using dihedral angle distributions and radial distribution function, *Heliyon 7, e08220*. https://doi.org/10.1016/j.heliyon.2021.e08220.

Lee, B., & Richards, F.M. (1971). The interpretation of protein structures: estimation of static accessibility. *Journal of molecular biology*, *55*(3), 379-IN4.

Lipinski, C.A., Lombardo, F., Dominy, B.W., & Feeney, P.J. (2012). Experimental and computational approaches to estimate solubility and permeability in drug discovery and development settings. *Advanced Drug Delivery Reviews*, *64*, 4-17. https://doi.org/10.1016/j.addr.2012.09.019.

Maharjan, R., Gyawali, K., Acharya, A., Khanal, M., Ghimire, M.P., & Lamichhane, T.R. (2024). Artemisinin derivatives as potential drug candidates against Mycobacterium tuberculosis: insights from molecular docking, MD simulations, PCA, MM/GBSA and ADMET analysis. *Molecular Simulation*, *50*(11), 1-12. https://doi.org/10.1080/08927022.2024.2346525.

Morris, G.M., Huey, R., Lindstrom, W., Sanner, M.F., Belew, R.K., Goodsell, D.S., & Olson, A.J. (2009). AutoDock4 and AutoDockTools4: Automated docking with selective receptor flexibility. *Journal of Computational Chemistry*, *30*(16), 2785-2791. https://doi.org/10.1002/jcc.21256.

Mukhtar, M., & Khan, H.A. (2023). Exploring the inhibitory potential of Nigella sativa against dengue virus NS2B/NS3 protease and NS5 polymerase using computational approaches. *RSC Advances*, *13*(27), 18306-18322. https://doi.org/10.1039/D3RA02613B.

Nguyen, V., Taine, E.G., Meng, D., Cui, T., & Tan, W. (2024). Chlorogenic Acid: A Systematic Review on the Biological Functions, Mechanistic Actions, and Therapeutic Potentials. *Nutrients*, *16*(7), 924. https://doi.org/10.3390/nu16070924.

Norahmad, N.A., Mohd Abd Razak, M.R., Mohmad Misnan, N., Md Jelas, N.H., Sastu, U.R., Muhammad, A., ... & Syed Mohamed, A.F. (2019). Effect of freeze-dried Carica papaya leaf juice on inflammatory cytokines production during dengue virus infection in AG129 mice. *BMC Complementary and Alternative Medicine*, *19*, 1-10. https://doi.org/10.1186/s12906-019-2438-3.

Obi, J.O., Gutiérrez-Barbosa, H., Chua, J.V., & Deredge, D. J. (2021). Current trends and limitations in dengue antiviral research. *Tropical Medicine and Infectious Disease*, *6*(4), 180. https://doi.org/10.3390/tropicalmed6040180.

Padilla-s, L., Rodríguez, A., Gonzales, M.M., Gallego-g, J.C., & Castaño-o, J.C. (2014). Inhibitory effects of curcumin on dengue virus type 2-infected cells in vitro. *Archives of Virology*, *159*, 573-579. https://doi.org/10.1007/s00705-013-1849-6.

Panya, A., Yongpitakwattana, P., Budchart, P., Sawasdee, N., Krobthong, S., Paemanee, A., ... & Yenchitsomanus, P.T. (2019). Novel bioactive peptides demonstrating anti-dengue virus activity isolated from the Asian medicinal plant Acacia catechu. *Chemical Biology &Drug Design*, *93*(2), 100-109. https://doi.org/10.1111/cbdd.13400.

Perera, R., & Kuhn, R.J. (2008). Structural proteomics of dengue virus. *Current Opinion in Microbiology*, *11*(4), 369-377. https://doi.org/10.1016/j.mib.2008.06.004.

Pintado Silva, J., & Fernandez-Sesma, A. (2023). Challenges on the development of a dengue vaccine: a comprehensive review of the state of the art. *Journal of General Virology*, *104*(3), 001831. https://doi.org/10.1099/jgv.0.001831.

Shabir, I., Kumar Pandey, V., Shams, R., Dar, A.H., Dash, K.K., Khan, S.A., ... & Pandiselvam, R. (2022). Promising bioactive properties of quercetin for potential food applications and health benefits: A review. *Frontiers in Nutrition*, *9*, 999752. https://doi.org/10.3389/fnut.2022.999752.

Tian, W., Chen, C., Lei, X., Zhao, J., & Liang, J. (2018). CASTp 3.0: computed atlas of surface topography of proteins. *Nucleic Acids Research*, *46*(W1), W363-W367. https://doi.org/10.1093/nar/gky473.

Valdés-Tresanco, M.S., Valdés-Tresanco, M.E., Valiente, P.A., & Moreno, E. (2021). gmx_MMPBSA: a new tool to perform end-state free energy calculations with GROMACS. *Journal of Chemical Theory and Computation*, *17*(10), 6281-6291. https://doi.org/10.1021/acs.jctc.1c00645.

Van Der Spoel, D., Lindahl, E., Hess, B., Groenhof, G., Mark, A.E., & Berendsen, H.J. (2005). GROMACS: fast, flexible, and free. *Journal of Computational Chemistry*, *26*(16), 1701-1718. https://doi.org/10.1002/jcc.20291.

Wahaab, A., Mustafa, B.E., Hameed, M., Stevenson, N. J., Anwar, M.N., Liu, K., ... & Ma, Z. (2021). Potential role of flavivirus NS2B-NS3 proteases in viral pathogenesis and anti-flavivirus drug discovery employing animal cells and models: a review. *Viruses*, *14*(1), 44. https://doi.org/10.3390/v14010044.

Watanabe, T., Arai, Y., Mitsui, Y., Kusaura, T., Okawa, W., Kajihara, Y., & Saito, I. (2006). The blood pressure-lowering effect and safety of chlorogenic acid from green coffee bean extract in essential hypertension. *Clinical and Experimental Hypertension*, *28*(5), 439-449. https://doi.org/10.1080/10641960600798655.

Yusof, R., Clum, S., Wetzel, M., Murthy, H.K., & Padmanabhan, R. (2000). Purified NS2B/NS3 serine protease of dengue virus type 2 exhibits cofactor NS2B dependence for cleavage of substrates with dibasic amino acids in vitro. *Journal of Biological Chemistry*, *275*(14), 9963-9969. https://doi.org/10.1074/jbc.275.14.996.

Zheng, W., Wu, H., Wang, T., Zhan, S., & Liu, X. (2021). Quercetin for COVID-19 and DENGUE co-infection: a potential therapeutic strategy of targeting critical host signal pathways triggered by SARS-CoV-2 and DENV. *Briefings in Bioinformatics*, *22*(6), bbab199. https://doi.org/10.1093/bib/bbab199.

Zoete, V., Cuendet, M. A., Grosdidier, A., & Michielin, O. (2011). SwissParam: a fast force field generation tool for small organic molecules. *Journal of Computational Chemistry*, *32*(11), 2359-2368. https://doi.org/10.1002/jcc.21816.